

Polysulfone and cellulose acetate-based membranes' potential application to photocatalytic membrane reactors

LUCIAN ALEXANDRU CONSTANTIN^{1*}, MIRELA ALINA CONSTANTIN¹,
 IOANA ALEXANDRA IONESCU¹, MARIA DIANA PUIU^{1,2}

¹National Research and Development Institute for Industrial Ecology – ECOIND, 57-73 Drumul Podu Dambovitei Street, 060652, district 6, Bucharest, Romania

²Faculty of Biology, University of Bucharest, 91-95 Splaiul Independentei, 050095, district 5, Bucharest, Romania

*Corresponding author: lucian.constantin@incdecoind.ro

Received:
17.11.2023

Accepted:
11.12.2023

Published:
20.12.2023

Abstract

Polysulfone (Psf) and Cellulose acetate (Ac-Cel) based membranes were synthesized via immersion precipitation – phase inversion techniques, starting from initial polymeric solutions with concentrations of 8%, 10% and 12%. Each membrane was characterized from morphological point of view by scanning electron microscopy and from compositional point of view by thermal analyses. Hydrodynamic characteristics were also determined for all membranes using both ultrapure water and real municipal wastewater. The results proved that polysulfone and cellulose acetate-based membranes are potential candidates to be used for advanced treatment of municipal wastewater using photocatalytic membrane reactors.

Keywords: polysulfone, cellulose acetate, municipal wastewater, wastewater treatment

INTRODUCTION

Municipal wastewater typically constitutes a significant portion of total wastewater globally. Municipal wastewater, also known as sewage or domestic wastewater, is generated from households, commercial establishments, and institutions, and includes water from toilets, sinks, showers, and other sources within urban and suburban areas. The volume of municipal wastewater is influenced by factors such as population density, urbanization, and water consumption patterns. Globally, an estimated 359.4×10^9 m³ of wastewater is produced annually, with 63% of it being collected, 52% being treated, while only a portion of around 11% of treated wastewater is being intentionally reused [1]. At this moment, 4% of wastewater generated globally is recovered and reused by membrane based processes [2].

Pressure driven processes such as microfiltration (MF), ultrafiltration (UF), nanofiltration (NF), reverse osmosis (RO) are used as polishing steps after the secondary treatment step for advanced wastewater treatment with 93% BOD (Biological Oxygen Demand) and 95% COD (Chemical Oxygen Demand) removal efficiencies [3]. The most common application of membranes for wastewater treatment is represented by the membrane bioreactor (MBR). MBR technology combines biological treatment (bioreactor) with membrane filtration, offering advantages such as high-quality effluent, a smaller footprint compared to conventional treatment processes, and the potential for water reuse. Several municipalities and industries around the world have adopted MBR technology for large-scale wastewater treatment. The use of MBRs is not limited to laboratory or pilot installations; instead, it has been increasingly applied in real-world scenarios. Full-scale MBR applications can be found in various settings, including municipal wastewater treatment, industrial wastewater treatment, water reuse projects and even containerized decentralized treatment systems.

However, the main drawback of membrane processes' large-scale adoption is represented by clogging and maintenance requirements [4, 5]. Thus, the majority of research works in the field performed on laboratory or pilot installations are focusing on delivering to industry better membrane materials that allow less intensive operation/maintenance effort [6, 7].

Polymeric membranes used for advanced treatment of municipal wastewater are starting from a large variety of polymers such as polysulfone (Psf), cellulose acetate (Ac-Cel), polyvinyl chloride, polyacrylonitrile etc. [8]. The most used technique for polymeric membrane preparation is represented by phase inversion technique via immersion – precipitation [9]. The preparation process involves the following steps: base polymer dissolution in a suitable solvent or mixture of solvents, polymeric solution deposition on flat or tubular surfaces, and phase inversion – polymer precipitation in a non-solvent bath [10].

The combination of photocatalysis with membrane processes is an area of research and development that holds great promise for green and sustainable wastewater treatment. This integrated approach combines the strengths of both technologies to address various pollutants and enhance the overall efficiency of water treatment thus combating potential risks to aquatic organisms and human health [11÷14]. The membrane is playing a double role in the process: recovery of suspended photocatalyst (in the case of slurry photocatalytic membrane reactor) as well as advanced removal of pollutants from the aqueous system. In this respect, the membrane should present excellent efficiencies in the removal of both suspended solids (TSS) and organic compounds (COD) [15÷17]. This was also the aim of the present study in which two types of polymers were used: Psf and Ac-Cel. Membranes were prepared via phase inversion starting from three polymeric solution concentrations: 8%, 10%, and 12%.

All membranes were characterised from a morphological and structural point of view and their hydrodynamic characteristics were determined (both average ultrapure water flow and separation flow). Two main indicators were monitored, namely organic loading (expressed as COD) and suspensions (expressed as TSM). Real municipal wastewater was used in all separation experiments. Moreover, clogging phenomena were monitored to assess membrane reusability potential as membrane fouling represents a critical parameter for photocatalytic membrane reactors (PMR) [18÷23].

EXPERIMENTAL PART

Synthesis of polymeric membranes

Two types of polymers were used: polysulfone (Psf) $M_w = 35000$ g/mol (Sigma Aldrich) and cellulose acetate (Ac-Cel) $M_w = 50000$ g/mol (Sigma Aldrich). 1-methyl 2-pyrrolidone (NMP), purity >99.5% (Merck) was used as solvent. Polyvinylpyrrolidone (PVP) K30 (40000 g/mol) – for Psf solution and K25 (24000 g/mol) – for Ac-Cel solution (both provided by Fluka) and polyethylene glycol (PEG) 400, $M=3500-4000$ g/mol (Scharlau) were used as additives. Ultrapure water obtained by using a Milli – Q Integral 15, Merck, Millipore equipment was used as a non-solvent within the coagulation bath. For post-treatment and conditioning of membranes ethanol 96% (Chimreactiv) and glycerine 99.5% (Chempur) were used.

Three types of membranes (starting from polymeric solutions with concentrations of 8%, 10%, and 12%) were obtained for each base polymer following the next steps (Fig.1):

- Dissolution of the polymer and additives within NMP under continuous stirring (for 24 h);
- Deposition of polymeric solution on flat glass sheet using a “doctor blade” type device (300 μ m slot);
- Immersion and precipitation to ultrapure water coagulation bath;
- Membrane post treatment and conditioning.

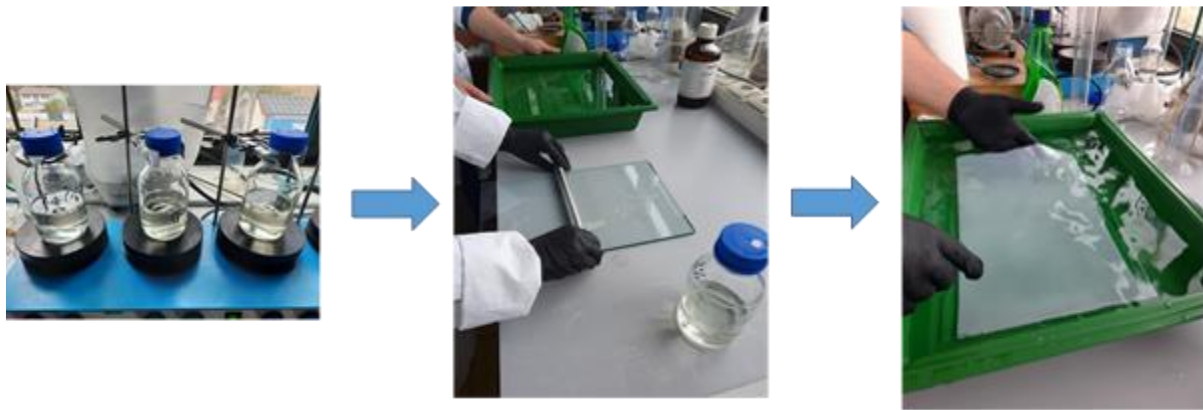


Fig. 1. Synthesis of polymeric membranes

Characterization of polymeric membranes

Obtained membranes were characterized from a morphological point of view by scanning electron microscopy using FEI Quanta FEG 250 equipment (Thermo Fischer) and from a structural point of view by thermal analyses using a STA 409 PCE equipment (Netszch). Hydrodynamic characterization of membranes was done by determination of average ultrapure water flow using a KMS Laboratory Cell – CF2 system (Koch Membrane Systems) and the following equation:

$$J_w = V/S \times t \quad (1)$$

where:

- J_w = ultrapure water flow through the membrane
- V = volume of ultrapure water passing through the membrane
- t = time in which volume V was collected
- S = effective membrane surface (28 cm^2)

Separation experimental setup

Separation experiments were realized using real wastewater sampled from a municipal wastewater treatment plant and the same KMS Laboratory Cell – CF2 used for the determination of hydrodynamic characteristics of membranes. Feed, concentrate and permeate volumes were monitored together with COD and TSM indicators. Four consecutive separation tests were performed for each membrane to assess membrane fouling and their reusability.

RESULTS AND DISCUSSION

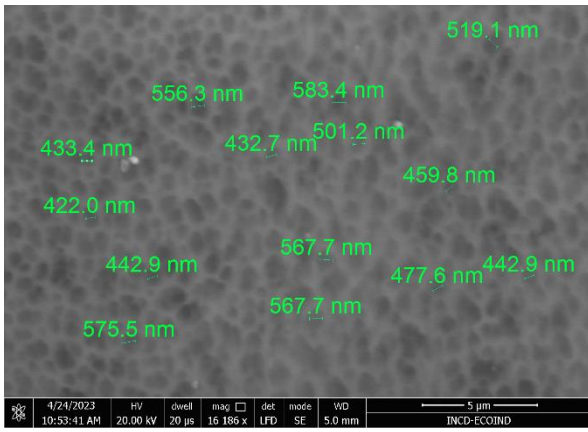
Morphological characterization of membranes

SEM images for Psf membranes (Fig. 2) revealed that at the active surface, pores are relatively uniformly distributed in the order 8% Psf > 10% Psf > 12% Psf with respect to the concentrations of polymeric solutions used for membrane fabrication. Thus:

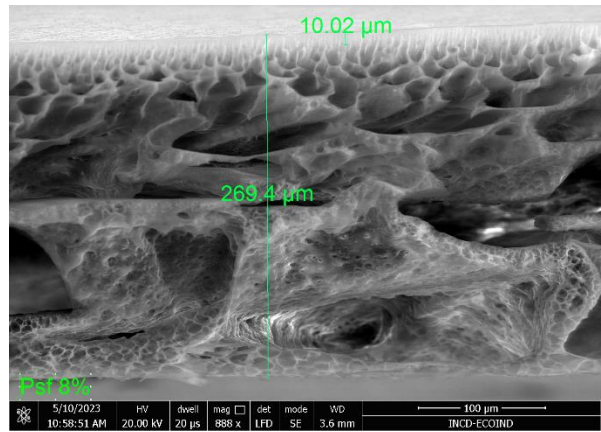
- Pore dimensions on active surface varied between $430 \div 600 \text{ nm}$ (8% Psf), $250 \div 350 \text{ nm}$ (10% Psf), and $145 \div 240 \text{ nm}$ (12% Psf)
- Total thickness of membranes varied between $270 \div 285 \text{ }\mu\text{m}$
- Active layer thickness varied between $2 \div 10 \text{ }\mu\text{m}$

On the other hand, SEM images for Ac-Cel membranes (Fig. 3) revealed also that at the active surface, pores are relatively uniformly distributed in the order 8% Ac-Cel > 10% Ac-Cel > 12% Ac-Cel with respect to the concentrations of polymeric solutions used for membrane fabrication (similar with Psf membranes). Thus:

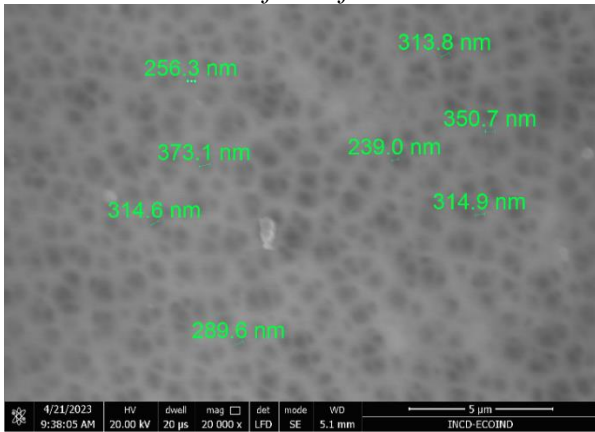
- Pore dimensions on active surface varied between $3.5 \div 5.6 \text{ }\mu\text{m}$ (8% Ac-Cel), $850 \text{ nm} \div 1.7 \text{ }\mu\text{m}$ (10% Ac-Cel), and $250 \div 500 \text{ nm}$ (12% Ac-Cel%)
- Total thickness of membranes varied between $165 \div 215 \text{ }\mu\text{m}$
- Active layer thickness varied between $1.5 \div 13.5 \text{ }\mu\text{m}$



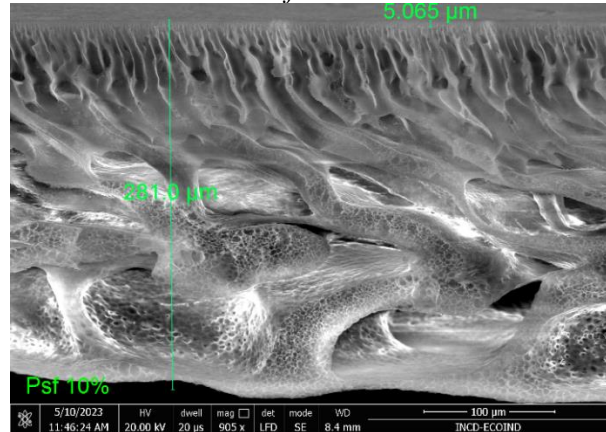
8% Psf - surface



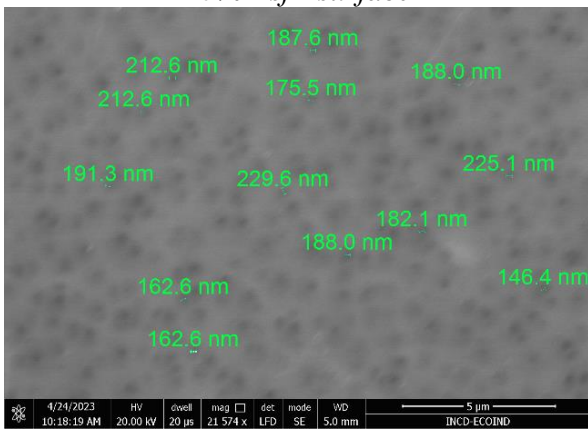
8% Psf - section



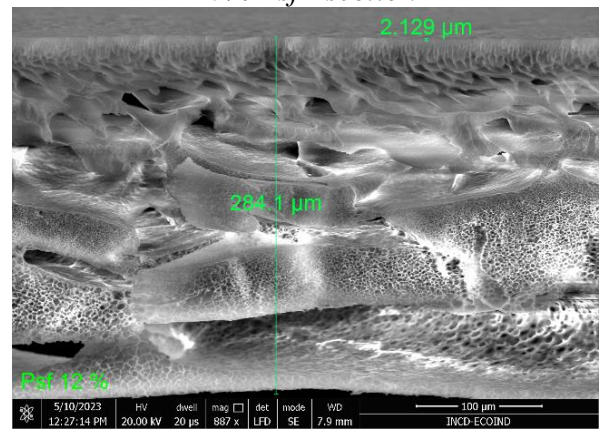
10% Psf - surface



10% Psf - section

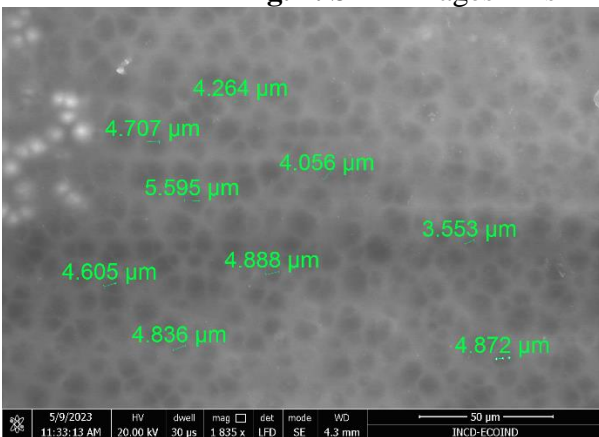


12% Psf - surface

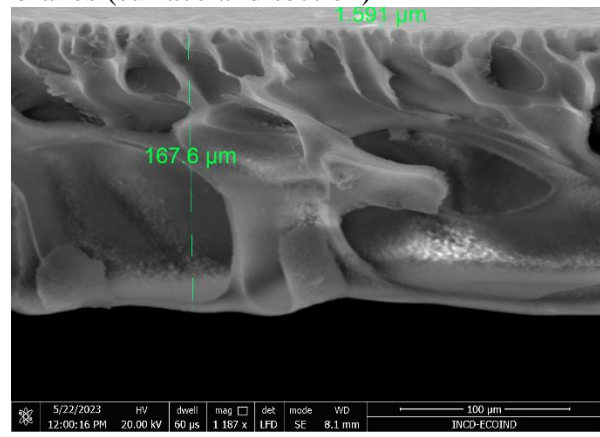


12% Psf - section

Fig. 2. SEM images – Psf membranes (surface and section)



8% Ac-Cel - surface



8% Ac-Cel - section

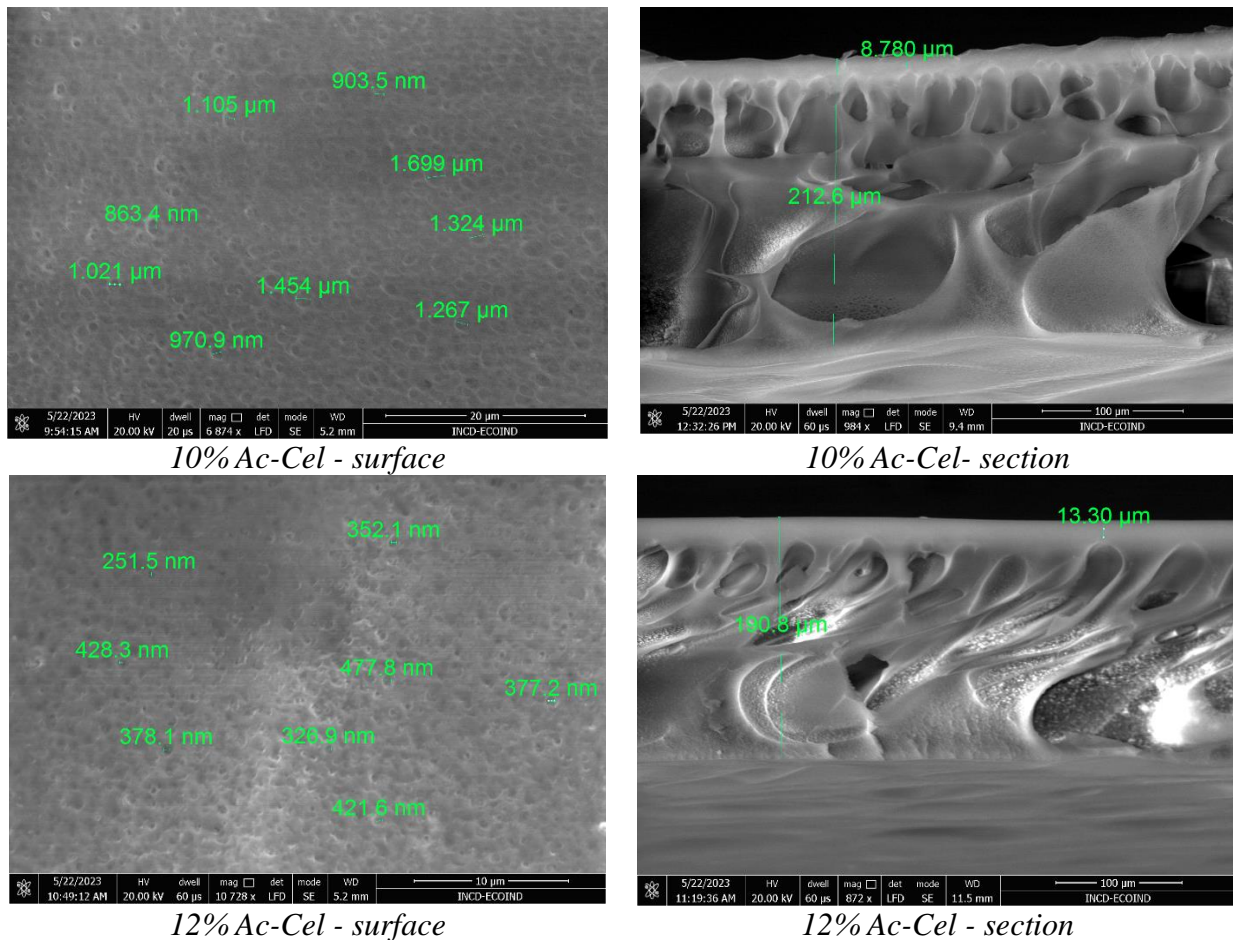


Fig. 3. SEM images – Ac-Cel membranes (surface and section)

Thermal analyses of membranes

Thermogravimetric analyses were performed for 12% membranes in comparison with the base polymer (Fig. 4, Fig. 5) and the obtained results confirmed membrane predicted composition. The small differences between membranes and related polymer thermographs can be explained by the presence of additives such as PEG and PVP.

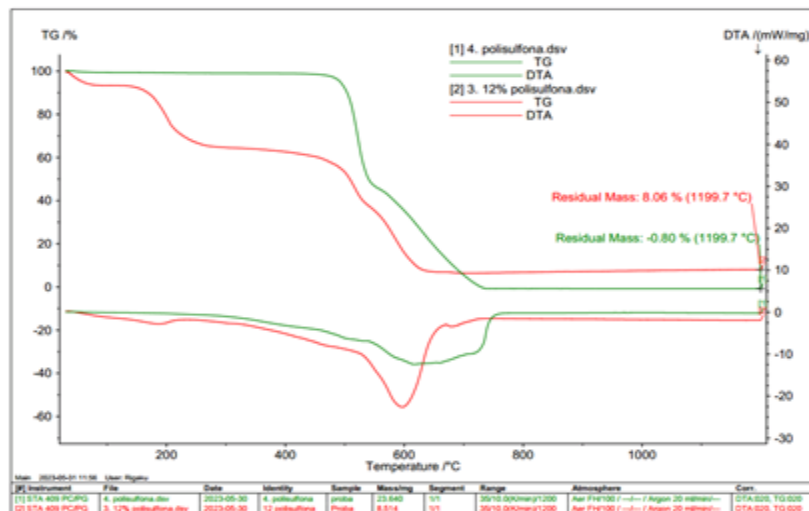


Fig. 4. Thermograph of 12% Psf membrane vs. Psf polymer

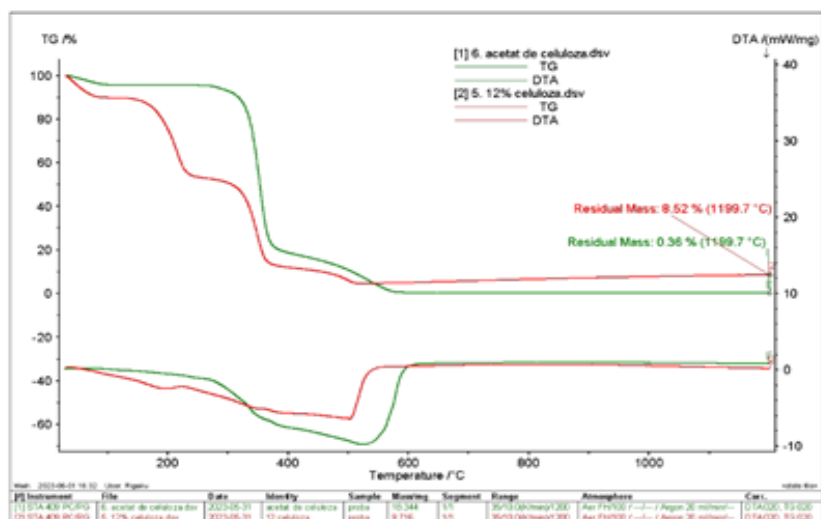


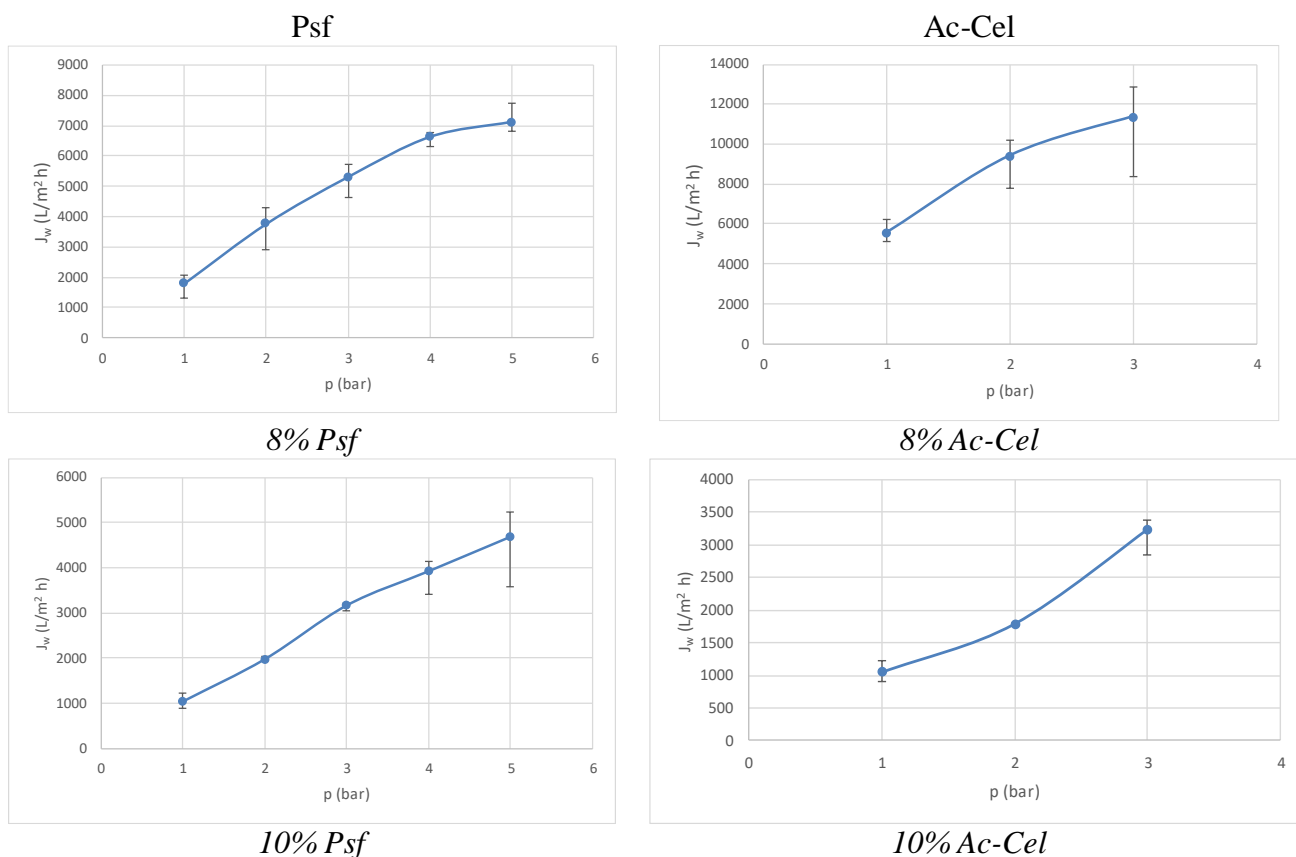
Fig. 5. Thermograph of 12% Ac-Cel membrane vs. Ac-Cel polymer

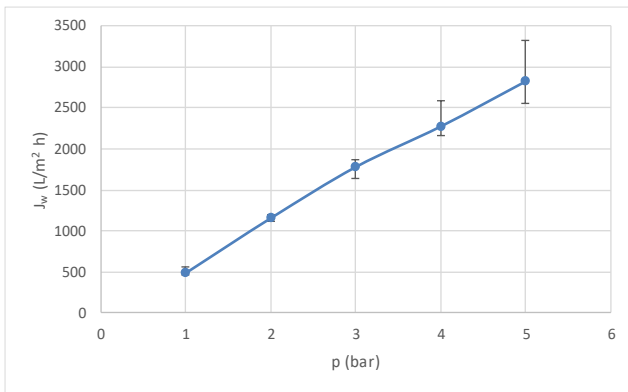
Determination of hydrodynamic characteristics

Average ultrapure water flow was determined for all types of membranes at various working pressures. The working pressure was varied within 1 to 5 bars domain for Psf membranes and within 1 to 3 bars for Ac-Cel membranes. Three determinations were performed for each membrane at a given pressure (Fig. 6).

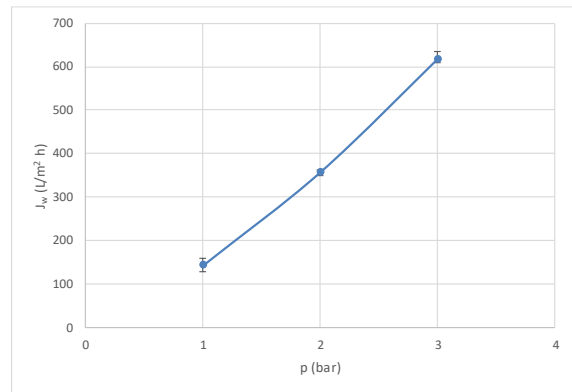
As was expected the average ultrapure water flow increases with the increase of the pressure and for both Psf and Ac-Cel membranes varied in the order 8% > 10% > 12% for a given pressure – following the concentration of polymeric solutions used for membrane’s fabrication.

For the separation experiments, a working pressure of 2 bars was chosen due to the good values of ultrapure water flows (for all membranes).





12% Psf

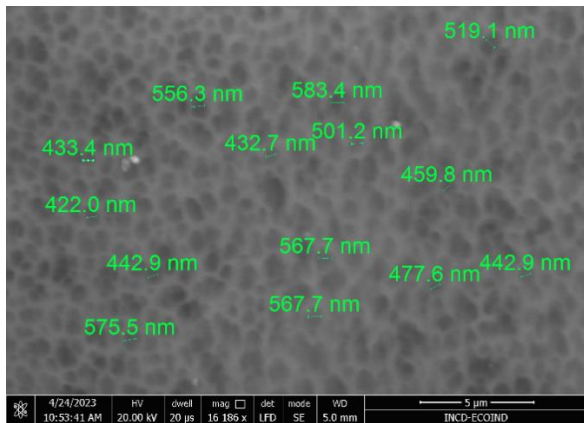


12% Ac-Cel

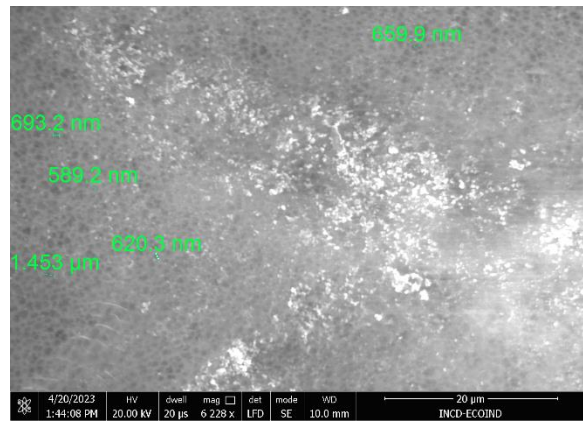
Fig. 6. Average ultrapure water flows vs. working pressure for Psf and Ac-Cel

Separation tests for membranes

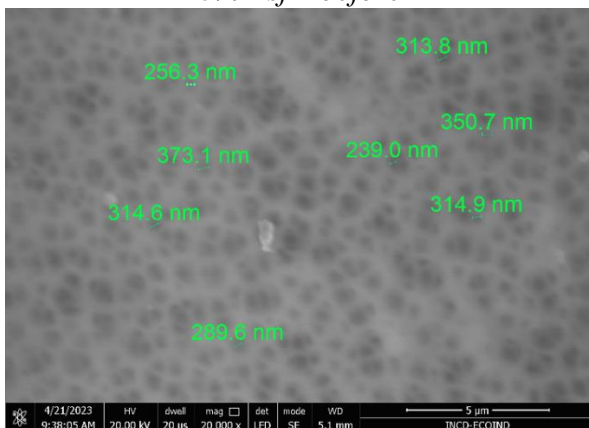
Four separation tests were performed for each membrane type at a working pressure of 2 bars. COD and TSM indicators were monitored to establish the separation efficiency of each membrane. After each separation, ultrapure water flow was determined to assess membrane fouling. Moreover, membranes after four separation tests were morphologically characterized by scanning electronic microscopy (SEM) (Fig. 7). Recorded SEM images confirmed the membrane's fouling and the fact that the dimensions of pores on the active surface of the membrane remains within the same dimensional domain.



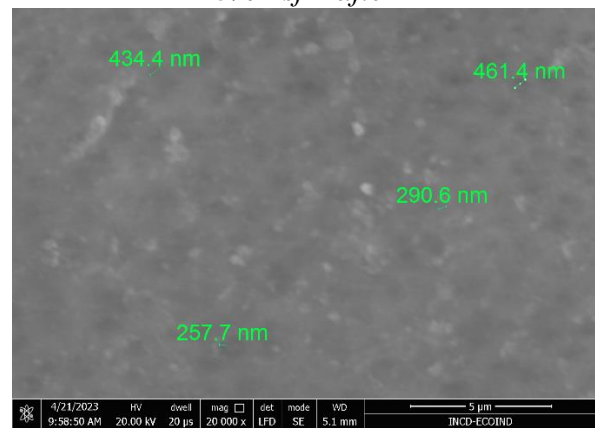
8% Psf – before



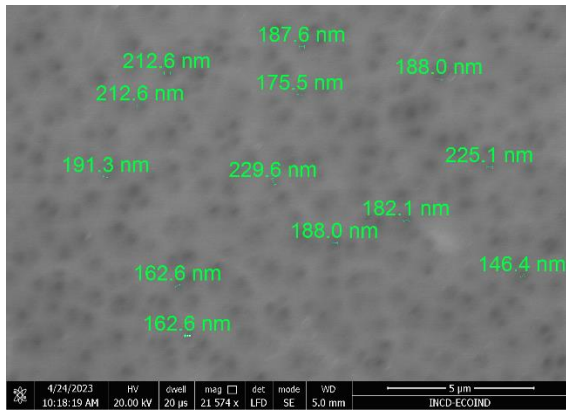
8% Psf – after



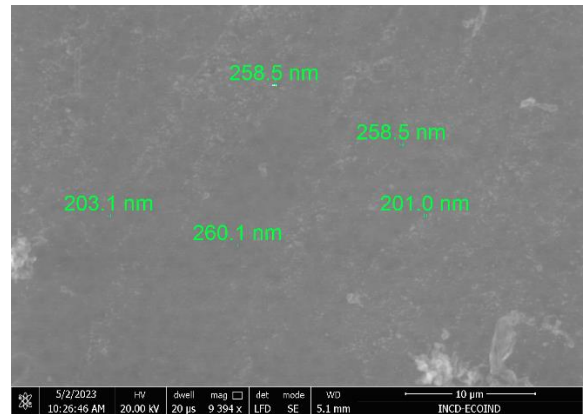
10% Psf – before



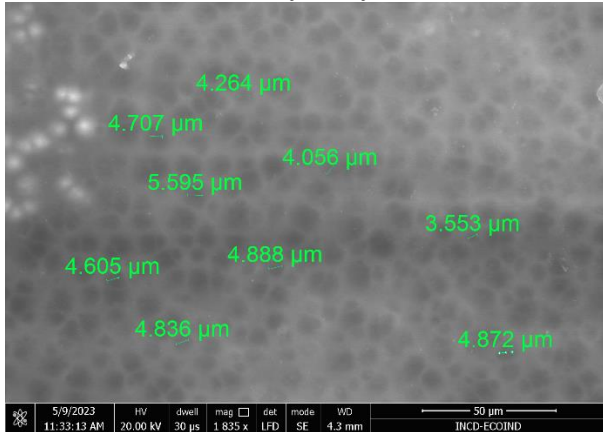
10% Psf – after



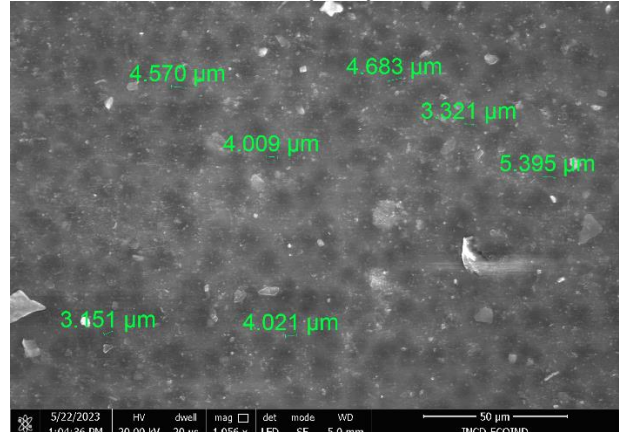
12% Psf – before



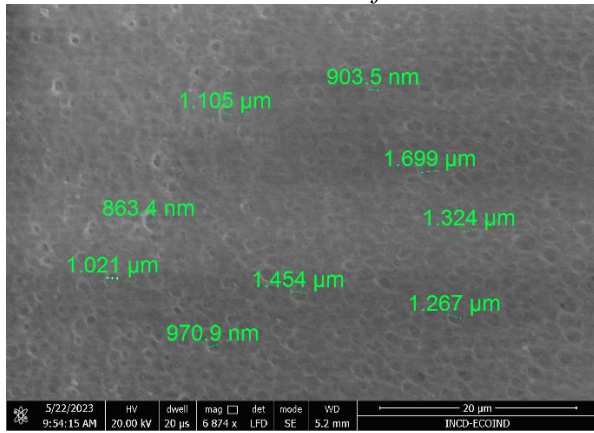
12% Psf – after



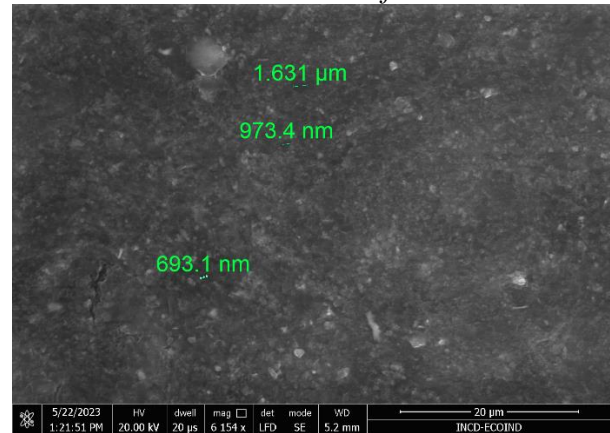
8% Ac-Cel - before



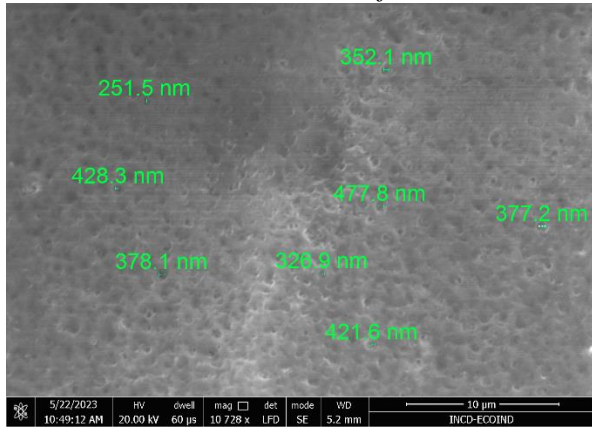
8% Ac-Cel – after



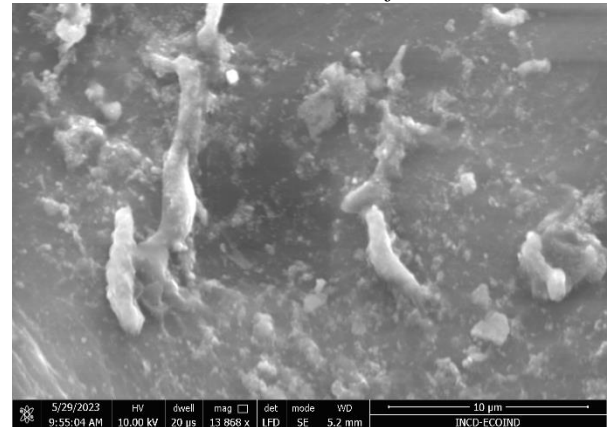
10% Ac-Cel - before



10% Ac-Cel – after



12% Ac-Cel - before



12% Ac-Cel – after

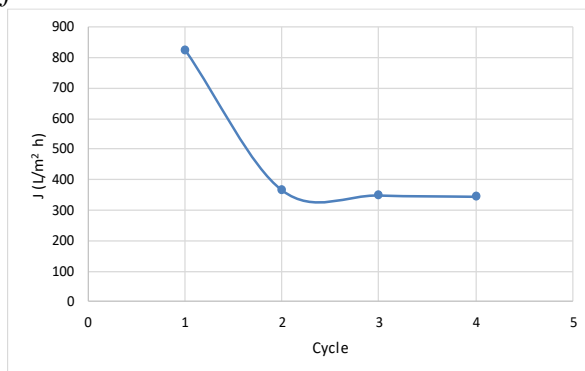
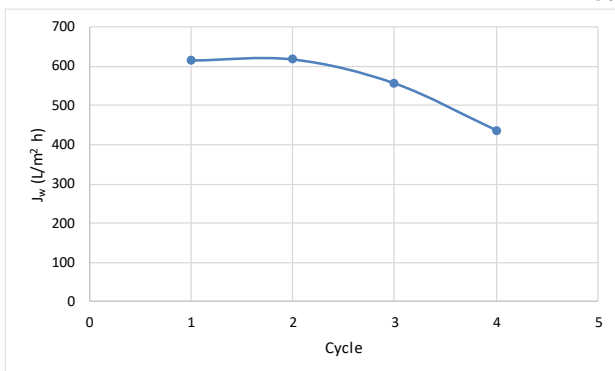
Fig. 7. SEM images for membranes before and after four separation tests for Psf and Ac-Cel

The membrane's fouling was also confirmed by the decrease of ultrapure water flows after each separation test as well as by the evolution of separation flows (Fig. 8).

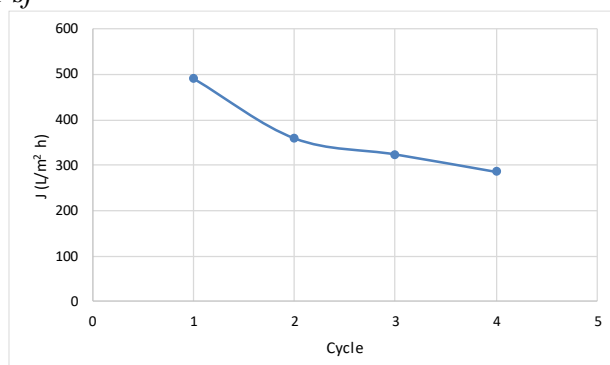
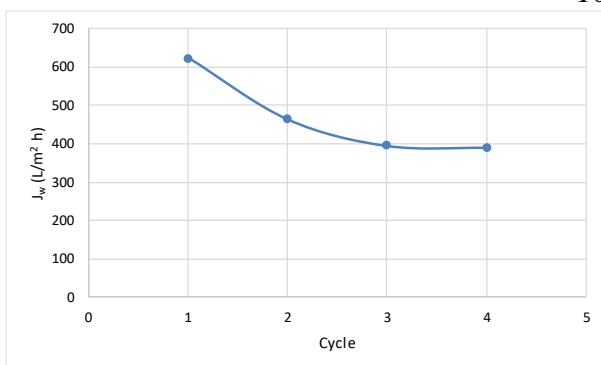
Ultrapure water flow

Separation flow

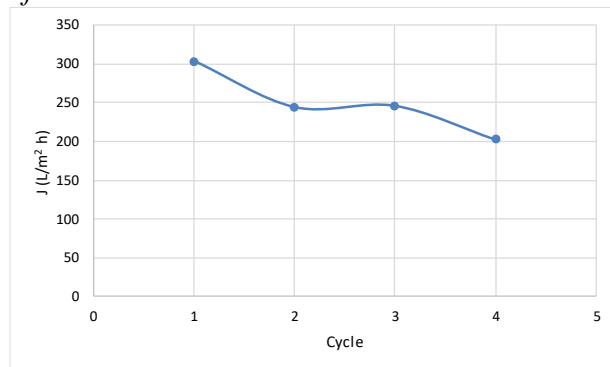
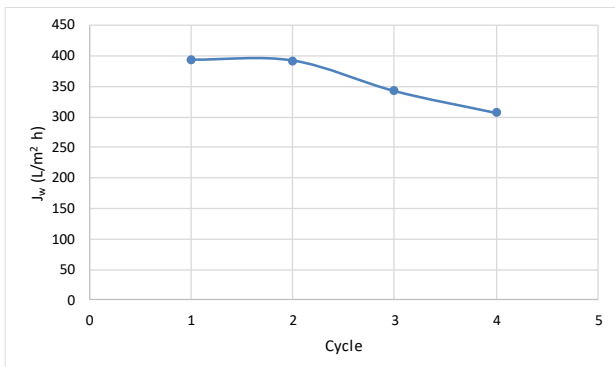
8% Psf



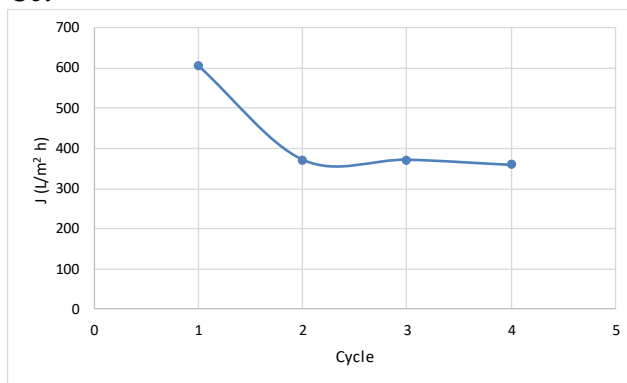
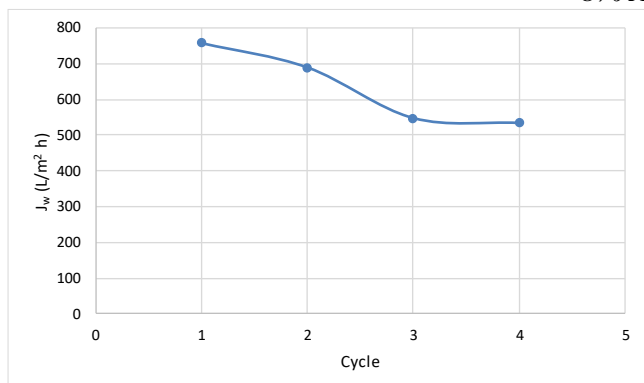
10% Psf



12% Psf



8% Ac-Cel



10% Ac-Cel

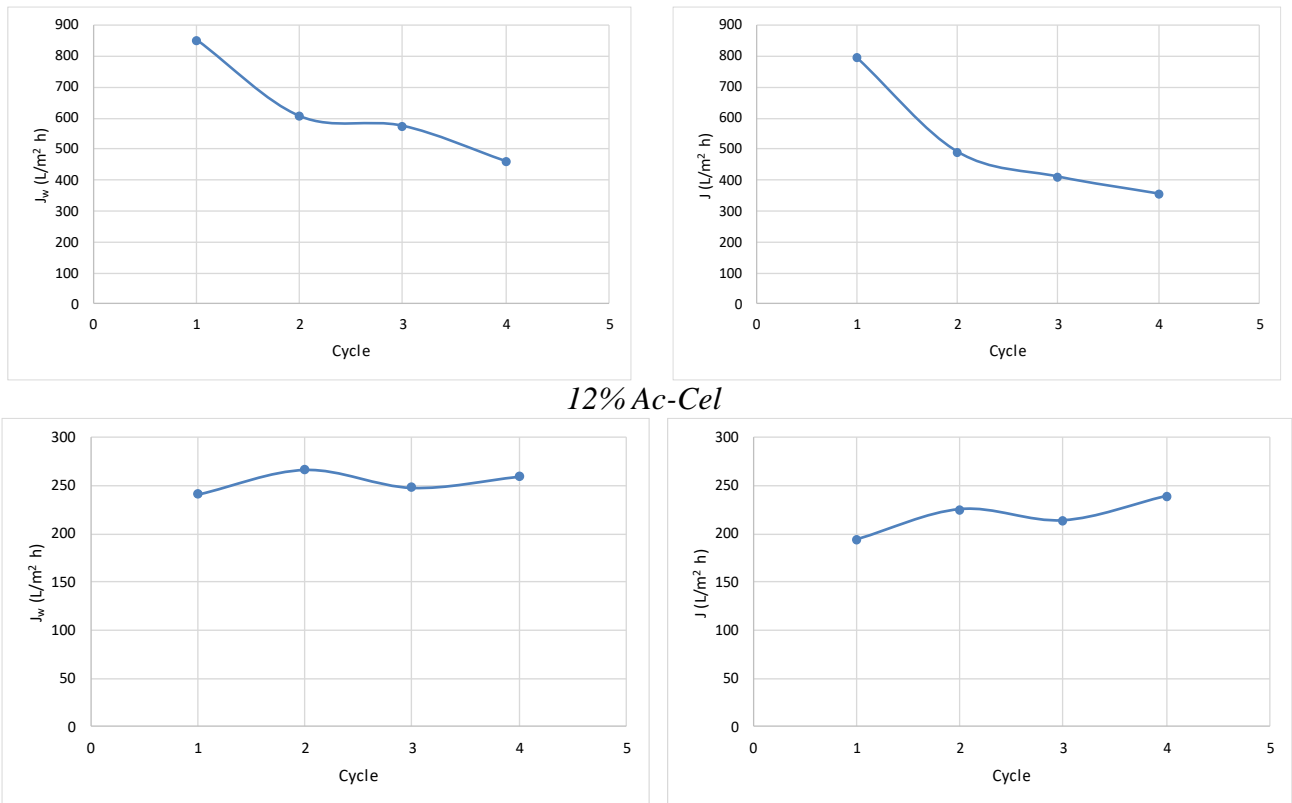


Fig. 8. Ultrapure water flow and separation flow vs. separation cycles for Psf and Ac-Cel

Recorded ultrapure water and separation flows proved that prepared membranes can be used at least for four consecutive separation cycles, registered flows being situated in the domain of microfiltration.

Regarding COD removal efficiencies, separation tests showed that the best results can be obtained in the case of Psf membrane for those obtained from polymeric solutions with 10% and 12% concentration, COD removal efficiencies being situated in the domain 62-72% for 10% Psf membrane and 64÷82% for 12% Psf membrane. In the case of Ac-Cel membranes, the best results for COD removal were obtained for the membrane prepared from 10% Ac-Cel polymeric solution reaching COD removal efficiencies of 89÷91% (Fig. 9)

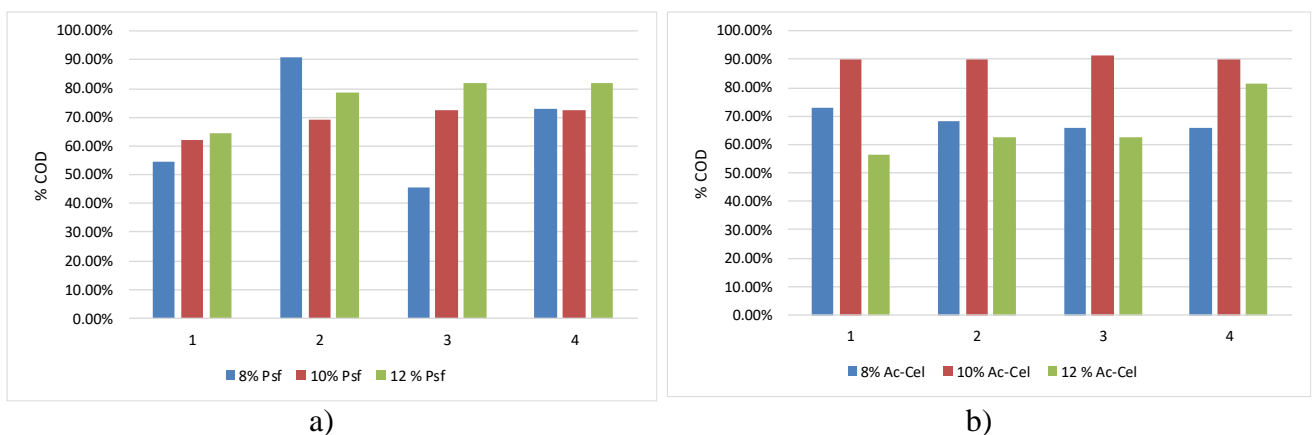


Fig. 9. COD removal efficiencies vs. separation cycle per each membrane type: a)Psf; b) Ac-Cel

In relation to TSM removal efficiencies, 10% and 12% Psf membranes led to residual TSM concentrations less than 5mg/L. The same result was obtained for Ac-Cel membranes obtained from polymeric solution with 10% and 12% Ac-Cel concentration (Fig. 10).

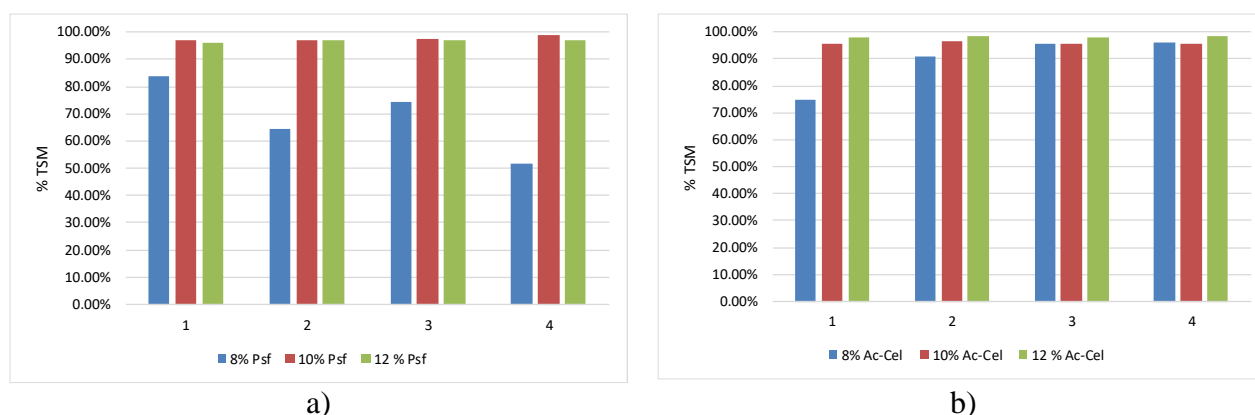


Fig. 10. TSM removal efficiencies vs. separation cycle per each membrane type : a)Psf; b) Ac-Cel

CONCLUSIONS

Polymeric membranes were synthesized via phase inversion techniques starting from Psf and AcCel solutions with concentrations of 8%, 10% and 12%. The concentration of the polymer in the casting solution is a critical factor. As expected, higher polymer concentrations result in denser membranes with smaller pores, as there is a higher polymer concentration available for phase separation.

The variation in pore sizes observed in the membranes produced using different polymers (Psf and Ac-Cel) and at different concentrations (8%, 10%, and 12%) can be attributed to several factors related to the inherent properties of polymers and processing conditions. Since the casting conditions were similar, the critical characteristics of the polymer that influence pore size include: polymer chemical structure, molecular weight and chain structure, solubility and viscosity.

The best results in terms of COD and TSM removal efficiencies were recorded for Psf and Ac-Cel membranes obtained from polymeric solutions with 10% and 12% concentration at a working pressure of 2 bars.

ACKNOWLEDGEMENTS

This work was carried out through the “Nucleu” Program within the National Research Development and Innovation Plan 2022-2027 with the support of Romanian Ministry of Research, Innovation and Digitalization, contract no.3N/2022, Project code PN 23 22 03 01.

REFERENCES

- [1] JONES, E.R., VAN VLIET, M.T.H., QADIR, M., BIERKENS, M.F.P., *Earth Syst. Sci. Data*, **13**, no. 2, 2021, p.237, <https://doi.org/10.5194/essd-13-237-2021>.
- [2] YANG, J., MONNOT, M., ERCOLEI, L., MOULIN, P., *Membranes*, **10**, no. 6, 2020, <https://doi.org/10.3390/membranes10060131>.
- [3] ABDEL-FATAH, M.A., SHAARAWY, H.H., HAWASH, S.I., *SN Appl. Sci.*, **1**, 2019, <https://doi.org/10.1007/s42452-019-1178-9>.
- [4] TANG, F., HU, H.-Y., SUN, L.-J., SUN, Y.X., SHI, N., CRITTENDEN, J.C., *Water Res.*, **90**, 2016, p. 329, <https://doi.org/10.1016/j.watres.2015.12.028>.
- [5] BATRINESCU, G., SCUTARIU, R.-E., NECHIFOR, G., IONESCU, I.-A., IANCU, V.-I., *J. Appl. Polym. Sci.*, **138**, no. 12, 2021, <https://doi.org/10.1002/app.50055>.
- [6] ZHAO, Y., QIU, Y., MAMROL, N., REN, L., LI, X., SHAO, J., YANG, X., VAN DER BRUGGEN, B., *Front. Chem. Sci. Eng.*, **16**, no. 5, 2022, p. 634, <https://doi.org/10.1007/s11705-021-2107-1>.
- [7] KLATT, M., BEYER, F., EINFELDT, J., *Water Sci. Technol.*, **86**, no. 9, 2022, p. 2213, <https://doi.org/10.2166/wst.2022.321>.
- [8] SCUTARIU, R.-E., BATRINESCU, G., NECHIFOR, G., IONESCU, I.-A., CRISTEA, N.-I., *U.P.B. Sci. Bull. Series B*, **83**, no. 1, 2021, p. 125.
- [9] BATRINESCU, G., CONSTANTIN, M.A., CUCIUREANU, A., NECHIFOR, G., *Polym. Eng. Sci.*, **54**, no. 7, 2014, p. 1640, <https://doi.org/10.1002/pen.23707>.

- [10] BATRINESCU, G., CUCIUREANU, A., BLAZIU-LEHR, C., 2010, RO1216195-B1.
- [11] MOLINARI, R., LAVORATO, C., ARGURIO, P., *Catalysts*, **10**, no. 11, 2020, <https://doi.org/10.3390/catal10111334>.
- [12] CONSTANTIN, L., NITOI, I., BATRINESCU, G., CRISTEA, I., NECHIFOR, G., Book 5 of 15th International Multidisciplinary GeoConferences SGEM, Albena, Bulgaria, 2015, p. 191.
- [13] CONSTANTIN, L., NITOI, I., CRISTEA, I., OANCEA, P., ORBECI, C., NECHIFOR, A.C., *Rev. Chim.*, **66**, no. 5, 2015, p. 597.
- [14] CONSTANTIN, L.A., CONSTANTIN, M.A., NITOI, I., CHIRIAC, F.L., GALAON, T., CRISTEA, N.I., *Rev. Chim.*, **69**, no. 11, 2018, p. 3234.
- [15] MARTINEZ, F., LOPEZ-MUNOZ, M.J., AGUADO, J., MELERO, J.A., ARSUAGA, J., SOTTO, A., MOLINA, R., SEGURA, Y., PARIENTE, M.I., REVILLA, A., CERRO, L., CARENAS, G., *Water Res.*, **47**, no. 15, 2013, p. 5647, <https://doi.org/10.1016/j.watres.2013.06.045>.
- [16] CHIN, S.S., CHIANG, K., FANE, A.G., *J. Membr. Sci.*, **275**, no. 1-2, 2006, p. 202, <https://doi.org/10.1016/j.memsci.2005.09.033>.
- [17] HUANG, M., CHEN, Y., HUANG, C.-H., SUN, P., CRITTENDEN, J., *Chem. Eng. J.*, **279**, 2015, p. 904, <http://dx.doi.org/10.1016/j.cej.2015.05.078>.
- [18] ZHANG, W., DING, L., LUO, J., JAFFRIN, M.Y., TANG, B., *Chem. Eng. J.*, **302**, 2016, p. 446, <https://doi.org/10.1016/j.cej.2016.05.071>.
- [19] KHADER, E.H., MOHAMMED, T.J., ALBAYATI, T.M., HARHARAH, H.N., AMARI, A., CATA SAADY, N.M., ZENDEHBOUDI, S., *Chem. Eng. Process.*, **192**, 2023, article no. 109503.
- [20] GOMAA, H.G., *Chem. Eng. Process.*, **193**, 2023, <https://doi.org/10.1016/j.cep.2023.109563>.
- [21] MOLINARI, R., LIMONTI, C., LAVORATO, C., SICILIANO, A., ARGURIO, P., *Chem. Eng. J.*, **451**, 2023, <https://doi.org/10.1016/j.cej.2022.138577>.
- [22] RATHNA, T., PONNANETTIYAPPAN, J., RUBENSUDHAKAR, D., *Environ. Technol. Inov*, **24**, 2021, <https://doi.org/10.1016/j.eti.2021.102023>.
- [23] CHEN, L., XU, P., WANG, H., *J. Hazard. Mater.*, **424**, 2022, <https://doi.org/10.1016/j.jhazmat.2021.127493>.

Citation: Constantin, L.A., Constantin, M.A., Ionescu, I.A., Puiu, M.D., Polysulfone and cellulose acetate-based membranes' potential application to photocatalytic membrane reactors, *Rom. J. Ecol. Environ. Chem.*, **2023**, 5, no. 2, pp. 5-16.



© 2023 by the authors. This article is an open access article distributed under the terms and conditions of the Creative Commons Attribution (CC BY) license (<http://creativecommons.org/licenses/by/4.0/>).